Direct Observation of Hindered Brownian Motion

Sherri A. Biondi and John A. Quinn
Dept. of Chemical Engineering, University of Pennsylvania, Philadelphia, PA 19104

Colloid phenomena can be studied from the perspective of a single particle or of a population of particles. The latter has been the traditional method used in observing Brownian behavior of suspended colloidal particles. In the particular case of restricted Brownian movement or hindered diffusion, macroscopic population observations introduce a number of secondary effects that need be accounted for in order to display the intrinsic behavior of the particles themselves. For example, data on hindered diffusion of micron-sized particles have been obtained by measuring net diffusive transport through well defined capillaries and porous membranes (see Deen, 1987, for a comprehensive review of this field). To reveal the underlying restricted transport behavior one must first account for factors such as equilibrium partitioning between bulk phase and pore, including steric restrictions; boundary layer effects at the pore entrance and exit; plus accompanying phenomena such as adsorption and osmotic flow (Malone and Anderson, 1978). Clearly, there are considerable benefits from direct observation of individual particle behavior. The attendant limitations are those of statistics and optical tracking artifacts. To extrapolate from individual behavior to transport properties, a number of events sufficient to guarantee statistical significance must be recorded. Also, observations of individual particles introduce measurement limitations associated with the field of vision and the ability to resolve time and position. Recent advances in video microscopy and automated image analysis enhance the perspective for direct observation of colloid behavior. Here we have demonstrated these techniques by measuring the hydrodynamic drag on micron-sized particles exhibiting Brownian movement in channels of comparable dimension.

Previous single particle measurements of Brownian motion have been carried out primarily using frame-by-frame motion picture photography taken through a microscope; measurements were made by filming individual diffusing particles. The film is projected as an enlarged image where the particle position can be tracked for each frame. From this map of the trajectory, the diffusion coefficient can be calculated directly. Perrin (1909), using a similar yet simplified version of this technique, verified the Stokes-Einstein equation for spherical Brownian particles. Suda and Imai (1985) examined rotational Brownian diffusion of elliptical WO_2 particles (length varying between four and ten micrometers). Vadas et al. (1976) verified the Stokes-Einstein equation for single latex spheres (Table 1) and determined the rotational diffusion coefficients of particle doublets. Despite the simplicity and accuracy of this technique, film projection is highly labor intensive and so has not been used extensively.

Improvements in image processing have made the measurement of particle displacement more efficient. A single colloidal particle can now be tracked so that the particle trajectory and diffusion coefficients are determined quickly and accurately. This diffusion coefficient is calculated directly and so errors arising from secondary effects and propagated calculation errors are eliminated. In this work, we demonstrate the application of image processing techniques to Brownian diffusion phenomena by tracking particles undergoing a random walk in both restricted and unrestricted geometries. Unhindered Brownian motion data are compared to the Stokes-Einstein equation and the hindered diffusion results are compared to existing hydrodynamic theories. In order to predict the particle motion, the theory of hindered diffusion is reviewed below.

Theory

The theory of hindered diffusion and the status of related research was the subject of a Journal Review by Deen (1987). Expressions for hindered diffusion coefficients have been determined for various geometries including cylindrical pores (Anderson and Quinn, 1974; Brenner and Gaydos, 1977) and slit geometries (Ganatos et al., 1980; Pawar and Anderson, 1993). Happel and Brenner (1965) rederived Faxen's expression to determine the ratio of hindered to unhindered diffusion coefficients D/D_∞ for a spherical particle diffusing between two parallel plates:

$$D/D_\infty = [1 - 1.004(a/h) + 0.418(a/h)^3 + \ldots] \qquad (1)$$

Since Eq. 1 is derived as a centerline approximation, it will underestimate the drag force experienced by the particle as it nears the wall. For this reason, the validity of the expression should be questioned at higher ratios of particle diameter to pore height (a/h). Deen (1987) reports that the error from

Correspondence concerning this article should be addressed to J. A. Quinn.

the centerline approximation should be 8% at $a/h = 0.1$ and 14% at $a/h = 0.5$. Recently, Pawar and Anderson (1993) derived a more accurate expression for diffusion in a slit geometry. They used asymptotic matching to relate the diffusion expressions in a region near the pore wall and a region near the centerline:

$$D/D_\infty = [1-(a/h)]^{-1}[1+9/16(a/h)\ln(a/h) - 1.194(a/h)+0.159(a/h)^3+\ldots] \quad (2)$$

It should be noted that both Faxen's and Pawar and Anderson's equations assume the hydrodynamic drag alone is hindering the motion of the particle and that electrostatic and other long-range interactions with the pore wall are negligible (note also that the effect of partitioning is not included in these theories). If the diffusing particle is continually within a few hundred angstroms of the pore wall or the ionic strength of the solvent is sufficiently small, these interactions can become an important factor. Several researchers (Malone and Anderson, 1978; Smith and Deen, 1983) have derived diffusion expressions which account for both hydrodynamic and specific particle/wall effects.

Experiments

Polystyrene latex beads (2, 3, and 9 μm diameter; Polyscience, Warrington, PA) were suspended in a solution of water, sucrose and NaCl at a particle concentration sufficiently small to ensure particle-particle interactions were negligible (particles were at least 5 particle dia. apart). The sucrose was added to keep the particles neutrally buoyant (s.g.1.0500 $\pm$ 0.0005 measured with a DMA 40 Digital Density Meter) while the NaCl (0.1M) was added to minimize electrostatic effects. The solution viscosity with the addition of the sucrose and salt was 1.48 cp. All experiments were conducted at room temperature 25°C. The particle solution was drawn into a rectangular channel (20, 30, 40 and 707 μm; tolerance $\pm$10%; Vitrodynamics, Rockaway, NJ) by capillary action and then sealed at both ends to minimize convection. The ratio of the capillary width to height was at least ten (for the 20, 30, and 40 μm channels) so that the rectangular channel walls could be treated as infinite parallel plates or, effectively, a two-dimensional (2-D) slit. The random motion of the particles in the slit was observed and tracked using the time lapse videomicroscopy system diagrammed in Figure 1.

Samples were mounted onto an inverted phase contrast microscope. Magnification in this system is possible up to 1,000 ×. A Hamamatsu Newvicon-tube C2400 videocamera (Photonic Microscopy Inc., Oak Brook, IL) was attached to the side of the microscope and connected to a JVC BR-9000U time-lapse videorecorder (JVC Company of America, Elmwood Park, NJ). The time-lapse feature on this videorecorder gives the user the option of choosing the number of frames recorded per second; for this study, videotaping was done in real time (30 frames/s). While monitoring a particle, the microscope was manually refocused to ensure that the center of the particle remained in the plane of focus. This provided a 2-D projection of the actual 3-D motion. A Series 151 image analysis system (Imaging Technology, Inc., Woburn, MA) was programmed to track approximately 200–300 particle centroid positions (x, y coordinates) on the video monitor (resolution 256×240 pixels or 120×91.2 μm). A detailed description of the tracking procedure follows.

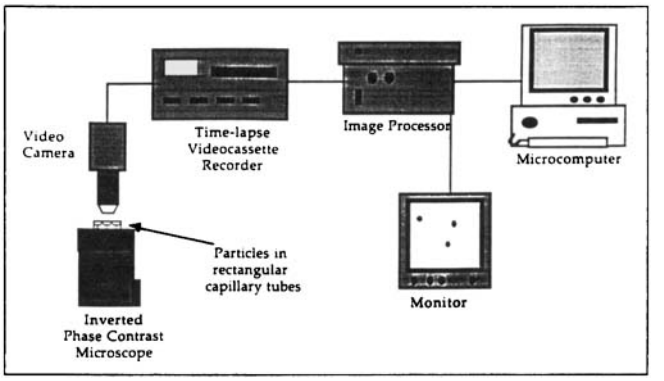

Figure 1. Experimental setup used to determine the trajectory of particles in bounded and unbounded environments.

In each experiment, the Einstein-Perrin relation:

$$\langle \Delta r^2 \rangle = 2 n_d D \Delta t \quad (3)$$

was used to determine the diffusion coefficient, where $\langle \Delta r^2 \rangle$ is the mean-squared displacement of the particle, D is the diffusion coefficient, t is time and n_d is the dimensionality of the system (Berg, 1983). More specifically, the following algorithm was used. The positions of an individual particle (r_1, r_2 ... r_N) were determined at specific times, t_1, t_2 ... t_N. For each value of $\Delta t = t_j - t_i$, the particle displacement $\Delta r = r_j - r_i$ was determined and squared Δr^2. The mean value of Δr^2 was determined for each Δt:

$$\langle \Delta r^2 \rangle = \Sigma(\Delta r^2)/N$$

where N is the number of displacements being averaged. For example, if the particle centroid is determined every second for 300 s, the particle displacement would be determined for each $\Delta t = t_2 - t_1 = t_3 - t_2 = t_j - t_{j-1} = 1$ s and then squared and averaged accordingly. This process would be repeated for $\Delta t = t_j - t_{j-2} = 2$ s and so on until $\Delta t = t_N - t_1 = 299$ s. Using Eq. 3 above, the diffusion coefficient can be determined by graphing $\langle \Delta r^2 \rangle$ and Δt (Figure 2). Since the dimensionality of the system is two, the diffusion coefficient will be the slope of this line divided by four. This method of determining the diffusion coefficients was used for all the measurements made, both hindered and unhindered.

Results

With unhindered geometries (0.5 mm^2 channels), it is expected that the diffusion coefficient obtained from the mean-square displacement data will match that calculated from the Stokes-Einstein equation. This is the case for the three particle sizes measured (Table 1).

For hindered geometries, the ratio of hindered to unhindered diffusion coefficients (D/D_∞) was determined and plotted as a function of the ratio of particle diameter to pore

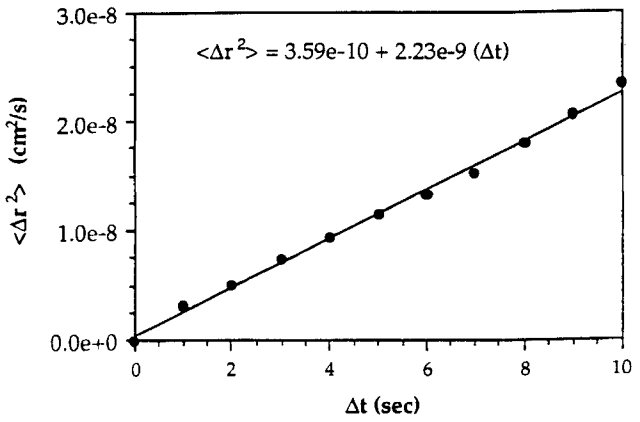

Figure 2. Mean-squared displacement vs. time for a 3 μm particle in a 30 μm channel.

The diffusion coefficient is determined from the slope to be 5.58×10^{-10} cm^2/s.

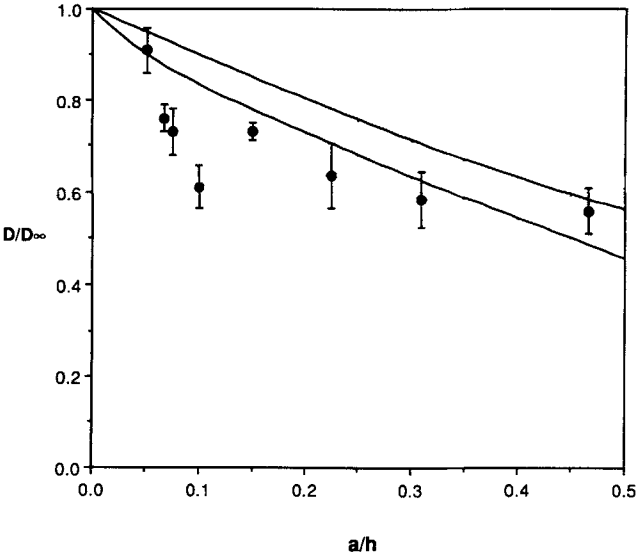

Figure 3. Hindered diffusion data from Table 2 plotted with Eqs. 1 (above) and 2 (below).

height a/h (Figure 3 and Table 2). For consistency, the value of D_∞ used to determine D/D_∞ was calculated from the particle radius using the Stokes-Einstein equation (Table 1). The theoretical curves in the plot are those discussed earlier: Faxen's expression (Eq. 1) and Pawar and Anderson's expression (Eq. 2). Faxen's equation should consistently overestimate the experimental data since the frictional drag expression that was employed always assumes that the particle is at the centerline (see Theory section). It is clear from Figure 3 that the data agree better with the theory of Pawar and Anderson; however, significant discrepancies between the two are apparent.

The theory of Pawar and Anderson is the most accurate model to date for hindered diffusion in a slit geometry because it accounts for the fact that a diffusing particle will sample all available positions over the entire pore height and therefore properly weights the average drag force experienced by a randomly moving particle. The observed discrepancy between the experimental data and this theory is most likely the result of the assumptions inherent in the data analysis. These include the possible effects of particle-wall interactions (the most significant being electrostatic forces), particle sedimentation and errors inherent in the time/trajectory sampling of individual particle motion.

Table 1. Unhindered Diffusion Coefficients

Particle Dia. (μm)	D (cm^2/s) Stokes-Einstein	D (cm^2/s) Exp.
Vadas (1976)		
1.19	4.12×10^{-9}	$4.26\ (\pm0.17)\times10^{-9}$
2.07	2.43×10^{-9}*	$2.47\ (\pm0.04)\times10^{-9}$
This Study		
2.06	1.43×10^{-9}*	$1.48\ (\pm0.04)\times10^{-9}$
3.01	0.98×10^{-9}	$1.02\ (\pm0.07)\times10^{-9}$
9.33	0.32×10^{-9}	$0.39\ (\pm0.05)\times10^{-9}$

The top values were obtained by Vadas et al. (1976) while the bottom values were determined in this study. The data are presented as mean ± standard deviation.

*Vadas et al. performed their experiments at a solution viscosity of 0.87 cp while the solutions used in this study had a viscosity of 1.48 cp.

The first assumption is that particle-wall interactions are negligible. These interactions become important only when a particle is continuously within tenths of micrometers from a wall and, for electrostatic interactions, the concentration of electrolyte is sufficiently low (Debye length of O(10^2 nm)). In the experiments performed here, these contributions should be negligible since the salt concentration was set at 0.1 M (a Debye length of approximately 1 nm (Russell et al., 1989); thus a ratio of Debye length to particle dia. ranging between 5×10^{-4} and 1×10^{-4}) and the particle was on average several micrometers from the wall.

A second assumption is that for a given time interval, sedimentation is small compared to the average Brownian displacement of a particle. This is the case if the potential energy associated with sedimentation [V_{part} (ρ_{fluid}-ρ_{part}) $g\Delta h$] is small compared to kT, the energy of thermal fluctuations. For the particle sizes used this potential energy of sedimentation could be of order kT; thus we cannot say that the diffusion coefficient is not influenced by sedimentation. For example, in these experiments, the settling velocity of a 9 μm particle would be approximately 10^{-2} μm/s (assuming the fluid-particle density difference is as great as the precision of fluid density measurement, viz. ±0.0005 g/cm^3). In 600 s this

Table 2. Hindered Diffusion Coefficients and Ratio of Hindered to Unhindered Diffusion Coefficients (D/D_∞) for Selected Particle Diameter to Slit Height Ratios (a/h)

a/h	D (cm^2/s)$\times10^{10}$	D/D_∞
2.06/40	13.0 ± 0.7	0.91 ± 0.05
2.06/30	10.8 ± 0.4	0.76 ± 0.03
3.01/40	7.19 ± 0.5	0.73 ± 0.05
3.01/30	5.96 ± 0.5	0.61 ± 0.05
3.01/20	7.14 ± 0.3	0.73 ± 0.02
9.33/40	2.03 ± 0.3	0.63 ± 0.07
9.33/30	1.87 ± 0.3	0.58 ± 0.06
9.33/20	1.80 ± 0.2	0.56 ± 0.05

Note: The data are presented as mean ± standard deviation.

particle would settle 6 μm and its root-mean-squared displacement by diffusion would be approximately 6 μm. Although sedimentation could contribute significantly to the displacement of the particle, its contribution is solely in the z-direction. Recall that no tracking is done in this direction; only the x-y Brownian movements are used to determine the diffusion coefficient. Sedimentation could affect the measurements indirectly by bringing the particle closer to the bottom wall (the particle to be tracked is usually chosen near the centerline and so the reverse situation of a particle settling away from the top wall will not exist) thus leading to a smaller diffusion coefficient.

A third assumption is that the particle samples all available vertical positions in the channel. There are several tracking approaches that can be followed. First, a large number of particles at a given height could be tracked for sufficiently short times to ensure that their height did not change appreciably during the time of observation. An average diffusion coefficient could be calculated at this height and, similarly, the process could be repeated at several other vertical positions. If the diffusion coefficients at the different elevations were averaged, an ensemble average over all height positions would result. This approach was not adopted as the number of tracked particles necessary for proper statistics would be too large for manual tracking. Second, one could determine a time-averaged diffusion coefficient by tracking a single particle for a time t; this would allow the particle to sample all the channel height positions. For example, if a 9 μm particle were diffusing within a 40 μm channel, the particle would need to diffuse 15.5 μm in the z (height) direction to sample all necessary positions (calculated as the distance from the channel centerline to the wall less the particle radius); the required time would be (from Eq. 3) approximately 4,000 s. This tracking procedure is also not feasible since the effect of settling/buoyancy could be appreciable over this time interval; given the density matching illustrated above, for long times ($> 10^3$ s) we could not guarantee that the particle had not gravitated towards a boundary wall. As an alternative to these two tracking techniques, n particles were tracked each for a time interval greater than t/n, and the data from the n particles were averaged to achieve an appropriate sampling. For example, in the case of the 9 μm particle referred to above, 10 particles were tracked, each for a time of approximately 600 s (equivalently 6,000 s of tracking). Many errors could be introduced in this tracking scheme. First, since the position of the particle is not known in the z-direction, one cannot guarantee that in 6,000 s, a particle would have sampled the entire pore height. Second, more than 10 particles need be tracked for the standard deviation in D/D_∞ to be small. It is likely that longer tracking times and a larger number of tracked particles would improve the accuracy of the measurements.

The error in the diffusion coefficient measurements has been attributed to three factors. Due to sedimentation, the particle trajectory is biased towards the wall and thus experiences greater drag than it would if it were precisely neutrally buoyant. Additionally, for each value of a/h the number of tracked particles was small (O(10)) and the net tracking time was only twice that needed to sample the channel height sufficiently. These latter two factors could result in poor statistics or biased sampling. Interestingly, the data at the extreme values of a/h are in better agreement with the theory than the intermediate points. Note that for increasing a/h, the probability that the center of a particle will occupy the entire nonsterically hindered region increases. For example, in a 20 μm pore, a 9 μm particle has less vertical space to traverse than does a 3 μm particle. Therefore, the 9 μm particle will sample the pore height more thoroughly and a more accurate value for the hindered diffusion coefficient should result. Conversely, as a/h approaches zero, the diffusion coefficient will approach D_∞. A 2 μm particle in a 40 μm channel will remain largely unaffected by the walls, and the calculated diffusion coefficients will be more representative of adequate sampling and less influenced by sedimentation.

Conclusion

An example of the use of image analysis as a tool for tracking individual Brownian particles has been presented. The precision of the technique is shown in the accuracy of the unhindered diffusion measurements. There are potential pitfalls inherent in the time/trajectory sampling of the particles and in gravitational effects due to particle/fluid density differences. To measure hindered diffusion coefficients accurately many particles need be tracked for sufficiently long times that the particle can sample the entire channel height. Our results show that hindered diffusion coefficients can be measured with reasonable accuracy (within 25% of theory) for short tracking times and a relatively small number of tracked particles.

The technique has applications beyond this demonstration. For example, measuring concentration effects, electrostatic interactions, diffusiophoresis and partitioning are obvious possible extensions. Also, the technique can be applied to microorganisms, so that the motility of bacteria (Phillips et al., 1994) and chemotactic movement can be studied.

Acknowledgment

The authors would like to thank Dr. John L. Anderson, Dr. William M. Deen, and Dr. Bret R. Phillips for helpful comments and suggestions.

Literature Cited

Anderson, J. L., and J. A. Quinn, "Restricted Transport in Small Pores. A Model for Steric Exclusion and Hindered Particle Motion," *Biophys. J.*, **14**, 130 (1974).

Berg, H. C., *Random Walks in Biology*, Princeton University Press, Princeton, NJ (1983).

Brenner, H., and L. J. Gaydos, "The Constrained Brownian Movement of Spherical Particles in Cylindrical Pores of Comparable Radius," *J. Colloid Interf. Sci.*, **58**, 312 (1977).

Deen, W. M., "Hindered Transport of Large Molecules in Liquid Filled Pores," *AIChE J.*, **33**, 1409 (1987).

Ganatos, P., R. Pfeffer, and S. Weinbaum, "A Strong Interaction Theory for the Creeping Motion of a Sphere Between Plane Parallel Boundaries: 2. Parallel Motion," *J. Fluid Mech.*, **99**, 775 (1980).

Happel, J., and H. Brenner, *Low Reynolds Number Hydrodynamics*, Prentice Hall, Englewood Cliffs, NJ (1965).

Malone, D. M., and J. L. Anderson, "Hindered Diffusion of Particles Through Small Pores," *Chem. Eng. Sci.*, **33**, 1429 (1978).

Pawar, Y., and J. L. Anderson, "Hindered Diffusion in Slit Pores—An Analytical Result," *I EC Res.*, 743 (1993).

Perrin, J., "Brownian Movement and Molecular Reality," Annales de Chimie et de Physique, 8eme Series, Taylor and Francis, London (1909).

Phillips, B. R., J. A. Quinn, and H. Goldfine, "Random Motility of

Swimming Bacteria: Single Cells Compared to Cell Populations," *AIChE J.*, **40**, 334 (1994).
Russel, W. B., D. A. Saville, and W. R. Schowalter, *Colloidal Dispersions*, Cambridge University Press, New York (1989).
Smith, F. G., and W. M. Deen, "Electrostatic Effects on the Partitioning of Spherical Colloids Between Dilute Bulk Solution and Cylindrical Pores," *J. Colloid Interf. Sci.*, **91**, 571 (1983).
Suda, H., and N. Imai, "Rotational Diffusion Constant of Microcrystals of Wolfram Oxide (WO_3) in Suspension," *J. Colloid Interf. Sci.*, **104**, 204 (1985).
Vadas, E. B., R. G. Cox, H. L. Goldsmith, and S. G. Mason, "The Microrheology of Colloidal Dispersions. II. Brownian Diffusion of Doublets of Spheres," *J. Colloid Interf. Sci.*, **57**, 308 (1976).

Manuscript received Feb. 25, 1994, and revision received July 5, 1994.